Frequency combs in quadratically nonlinear resonators

Miro Erkintalo[1,*], Tobias Hansson[2,3], Iolanda Ricciardi[4], Stéphane Coen[1], Maurizio De Rosa[4], Stefan Wabnitz[3,4], and François Leo[1]

[1]*The Dodd-Walls Centre for Photonic and Quantum Technologies, Department of Physics, The University of Auckland, Auckland 1142, New Zealand*
[2]*Department of Applied Physics, Chalmers University of Technology, SE-41296 Göteborg, Sweden*
[3]*Dipartimento di Ingegneria dell'Informazione, Università di Brescia, via Branze 38, 25123 Brescia, Italy*
[4]*CNR-INO, Istituto Nazionale di Ottica, Via Campi Flegrei 34, 80078 Pozzuoli (NA), Italy*
[*]*m.erkintalo@auckland.ac.nz*

Abstract: We describe the physics and modelling of frequency combs and corresponding temporal patterns in coherently driven, quadratically nonlinear resonators.

OCIS codes: 190.4975 Parametric processes, 230.5750 Resonators.

High-Q microresonators driven with continuous wave (cw) lasers have recently emerged as an attractive new platform for the generation of coherent optical frequency combs [1]. They possess the ability to create frequency combs with very large line spacing and power per mode, thus making them suitable for a diversity of applications that cannot easily be accessed using conventional mode-locked laser frequency combs [2].

Microresonator frequency combs studied to date arise via third-order optical "Kerr" nonlinear effects [3]; the underlying physics is intimately related to dynamics of coherently-driven fibre ring resonators [4]. Unfortunately, third-order effects do not easily permit the creation of frequency combs in particular key regions of the electromagnetic spectrum: material dispersion obstructs the creation of combs in the visible, whilst access to mid-infrared demands for complex and expensive pump sources. Access to those spectral regions could be viable by leveraging second-order $\chi^{(2)}$ nonlinear interactions, such as second-harmonic generation and/or parametric down-conversion. Experiments in silicon nitride [5] and aluminium nitride [6] microresonators have indeed demonstrated that a weak $\chi^{(2)}$ can lead to the intracavity conversion of a Kerr frequency comb to shorter wavelengths. More significantly, however, experiments in *bulk* free-space cavities have demonstrated that frequency combs can arise *purely* through second-order $\chi^{(2)}$ nonlinear effects [7, 8], thereby alluding to a fundamentally new paradigm of frequency comb generation. The exploration of this new paradigm calls for theoretical models that can accurately describe the underlying physics. Although many theoretical studies have been reported on cw-driven quadratically nonlinear cavities, the investigations have hitherto involved only a small number (typically up to 4) frequency components, or explored parameter regimes that may not be relevant for realistic dispersive systems.

In this talk, we present model equations that enable accurate numerical studies and concise theoretical analysis of frequency comb generation in dispersive, quadratically nonlinear resonators [9, 10]. We apply our models to the particular case of frequency comb generation in intracavity SHG, where experiments have recently been reported [8], and obtain simulation results that are in excellent agreement with measurements. Our study reveals that the onset of frequency comb formation is activated by the large walk-off between the fundamental and the second-harmonic fields.

We consider slowly-varying electric field envelopes A and B centred at ω_0 and $2\omega_0$, circulating in a dispersive ring resonator that is driven with a cw field $A_{\rm in}$ at ω_0. We assume, for simplicity, that the resonator is made entirely of a $\chi^{(2)}$ medium with length L, that the SHG process $\omega_0+\omega_0=2\omega_0$ is almost phase-matched, and that the resonator has high finesse (at least) around the fundamental frequency. We have found that, under these conditions, the second-harmonic field is dynamically slaved to the fundamental field across a wide range of realistic conditions [9, 10]. Moreover, restricting the more general $\chi^{(2)}$ model equations to the case of intracavity SHG, we have derived the following mean-field equation for the the field envelope at the fundamental frequency:

$$t_{\rm R}\frac{\partial A(t,\tau)}{\partial t}=\left[-\alpha-i\delta_0+iL\sum_{k\geq 2}\frac{\beta_k}{k!}\left(i\frac{\partial}{\partial\tau}\right)^k\right]A-(\kappa L)^2A^*\left[A^2(t,\tau)\otimes I(\tau)\right]+\sqrt{\theta}A_{\rm in}. \quad (1)$$

Here $t_{\rm R}$ is the roundtrip time, α represents half the total cavity losses at ω_0, $\delta_0=2\pi l-\phi_0$ is the phase detuning of the driving field with respect to the closest cavity resonance (with order l), β_k are the dispersion coefficients around

ω_0, and θ is the power transmission coefficient of the coupler used to inject the driving field A_{in} into the cavity. The continuous variable t is a *slow time* that measures the evolution of the field envelope over several roundtrips, whilst τ is a *fast time* variable that allows for the description of the field profile. κ describes the strength of the quadratic nonlinearity, $\otimes$ denotes convolution and $I(\tau)$ is a nonlinear response function that incorporates the resonant cavity configuration as well as the interaction with the second-harmonic field (including walk-off). Notably, the functional form of $I(\tau)$ is different for singly and doubly resonant cavity constructions (see [9] and [10] for details).

Equation (1) governs the temporal and spectral dynamics of intracavity SHG. We have confirmed its validity by comparing its predictions against experimental observations reported in a singly resonant free-space intracavity SHG system. To this end, Fig. 1 shows experimentally measured [8] and numerically simulated spectra around the fundamental frequency for two different sets of cavity parameters (see [9]). Clearly, the simulation results are in excellent quantitative agreement with experimental observations, thus corroborating the validity of Eq. (1). At this point we remark that the individual comb lines are not visible in Figs. 1(b) and (d) due to their dense 493 MHz spacing.

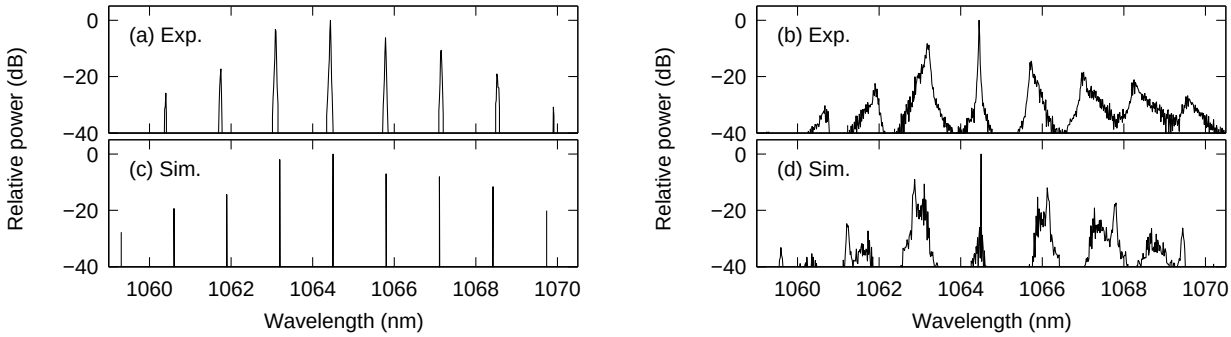

Fig. 1. (a, b) Experimentally measured spectra around the fundamental frequency in a singly resonant cavity SHG system (adapted from [8]). (c, d) Corresponding results from numerical simulations. The pump-cavity parameters are different in (a, c) and (b, d). For more details, see [9].

Closer analysis of the simulation results reveals that the comb formation initiates from a modulation instability (MI) that is driven by the well-known "internally-pumped" OPO process [8]. To gauge the conditions under which MI (hence, comb formation) manifests itself, we have also examined the linear stability of Eq. (1). Our analysis shows that the temporal walk-off between the fundamental and the second-harmonic fields plays a decisive role in the MI dynamics. For example, in the singly-resonant case, we find that MI only emerges for sufficiently large walk-off values.

In conclusion, we have theoretically examined the generation of frequency combs and corresponding temporal patterns in dispersive, quadratically nonlinear cavities [9, 10]. Considering cavity-enhanced SHG as a representative example, we have derived a single mean-field equation that describes the intracavity dynamics. Results from numerical simulations show excellent agreement with experimental observations. Although we have focussed on intracavity SHG, we expect our general equations and results to resonate across various configurations.

References

1. P. Del'Haye, A. Schliesser, O. Arcizet, T. Wilken, R. Holzwarth, and T. J. Kippenberg, Nature **450**, 1214 (2007).
2. T. J. Kippenberg, R. Holzwarth, and S. A. Diddams, Science **332**, 555 (2011).
3. Y. K. Chembo, D. V. Strekalov, and N. Yu, Phys. Rev. Lett. **104**, 103902 (2010).
4. S. Coen, H. G. Randle, T. Sylvestre, and M. Erkintalo, Opt. Lett. **38**, 37 (2013).
5. S. Miller, K. Luke, Y. Okawachi, J. Cardenas, A. L. Gaeta, and M. Lipson, Opt. Express **22**, 26517 (2014).
6. H. Jung, R. Stoll, X. Guo, D. Fischer, and H. X. Tang, Optica **1**, 396 (2014).
7. V. Ulvila, C. R. Phillips, L. Halonen, and M. Vainio, Opt. Lett. **38**, 4281 (2013).
8. I. Ricciardi, S. Mosca, M. Parisi, P. Maddaloni, L. Santamaria, P. De Natale, and M. De Rosa, Phys. Rev. A **91**, 063839 (2015).
9. F. Leo, T. Hansson, I. Ricciardi, M. De Rosa, S. Coen, S. Wabnitz, and M. Erkintalo, Phys. Rev. Lett. **116**, 033901 (2016).
10. F. Leo, T. Hansson, I. Ricciardi, M. De Rosa, S. Coen, S. Wabnitz, and M. Erkintalo, Phys. Rev. A **93**, 043831 (2016).